Gregor A. Scheffler

Xella Technologie- und Forschungsgesellschaft, Section of Applied Research and Building Physics, Hohes Steinfeld 1, 14797 Kloster Lehnin, Germany

Introduction of a full-range model for liquid and vapor transport properties of autoclaved aerated concrete

ABSTRACT: The hygric performance of autoclaved aerated concrete is a key determinant for many other material properties as e.g. thermal conduction, carbonation or shrinkage behavior. Laboratory determination of hygric material properties, i.e. moisture storage and moisture transport, is hence a prerequisite and a standard in production and process supervision.

In this context, prediction and simulation of the hygric material performance based on numerical calculation models has become a widely used research and design tool. However, for assessment of the material behavior under variable climatic conditions, the hygric material properties have to be determined in a first step. In a second step, these properties have to be transformed into the non-linear coefficients required by these numerical calculation models.

This paper is the second of two focusing on the second step. It introduces a full-range hygric material model bridging the gap between measured material properties and the non-linear storage and transport coefficients in the transfer equation. The model is based on the conductivity approach and relies on a bundle of tubes approach to derive the transport function from the pore structure of the material. By extending this approach with a mechanistic treatment of serial and parallel structured transport, a semi-empirical material model is developed providing a high flexibility and adjustability.

The model is applied for an aerated autoclaved concrete. Input data are basic material properties obtained by the methods introduced in the first paper [26]. The approximation procedure is described and the achieved accuracy is discussed. In conclusion, the model is very suitable for sophisticated research as well as for a broad application to autoclaved aerated concrete in particular, and to porous materials in general.

KEY WORDS: moisture storage, moisture transport, modeling

1. Introduction

Within the past decades, the numerical simulation of heat and moisture transport phenomena has become a widely accepted and commonly applied investigation method. Many tools have been developed [10, 11, 13, 15, 18] and both extended and improved [16, 22].

To obtain meaningful results though, the boundary conditions and material properties have to be modeled and accounted correctly, too. Whereas recent studies dealt with boundary condition modeling and incorporation [3, 4, 9, 17], the modeling of moisture transport properties appears to be not in the focus of current research. This paper addresses the modeling of hygric material behavior for numerical simulation.

Hygric material modeling depends on the general transport theory. The derivation of the balance and constitutive equations for moisture transport can be found in the literature, among others in [2, 6, 7, 11, 13, 19]. However, for a better understanding, the transport equation shall be briefly introduced.

According to their driving forces, liquid and vapor flow are treated separately. Together they yield the transport equation of moisture. The vapor diffusion flow is proportional to the vapor pressure gradient with the vapor permeability $D_V(\theta_l)$ (m^2/s) as transport coefficient. The liquid water flow is proportional to the capillary pressure gradient ∇p_c. The corresponding transport coefficient is the liquid water conductivity $K_l(\theta_l)$ (s). It depends as well as the vapor permeability of the porous medium and is typically expressed as function of the moisture content.

$$\frac{\partial m_{l+v}}{\partial t} = -\nabla\left(\frac{D_v(\theta_l)}{R_v \cdot T}\nabla p_v + K_l(\theta_l)\cdot\left[\nabla p_c + \rho_w \cdot g\right]\right) \qquad (1)$$

Material modeling has to deal with the vapor transport coefficient $D_V(\theta_l)$ (m^2/s), the liquid transport coefficient $K_l(\theta_l)$ (s), and the moisture capacity $\theta_l(p_c)$. All of them show significant moisture dependence. The moisture capacity as the relation of moisture content and moisture potential can be measured throughout the whole moisture range and requires only a reasonable functional description. The transport coefficients can be measured only at very high or very lo w moisture contents. The overall functional description must be modeled. Hence, this paper focuses on the modeling of the transport coefficients of liquid and vapor.

The paper introduces a recently developed material model [24, 25]. It is applicable for the whole range of moisture contents with a high degree of flexibility and accuracy. The model can be extended to hysteresis and salt transport modeling.

A bundle of tubes description was chosen as the model basis. It is coupled with a mechanistic model distinguishing between serial and parallel moisture transport in both the vapor and the liquid phase. By that, the connectivity of both phases is accounted for introducing an additional saturation dependency for both transport

coefficients. As result, the developed model allows flexible adjustment throughout the whole range of moisture contents while it is still relatively simple to be applied. The model is therefore suitable for a general application to porous materials.

2. Whole range material model

Hygric material modeling has to deal with the moisture transport and the moisture storage characteristics. The corresponding transport coefficients are the vapor permeability $D_v(\theta_l)$ (s) and the liquid conductivity $K_l(\theta_l)$, both functions of the moisture content.

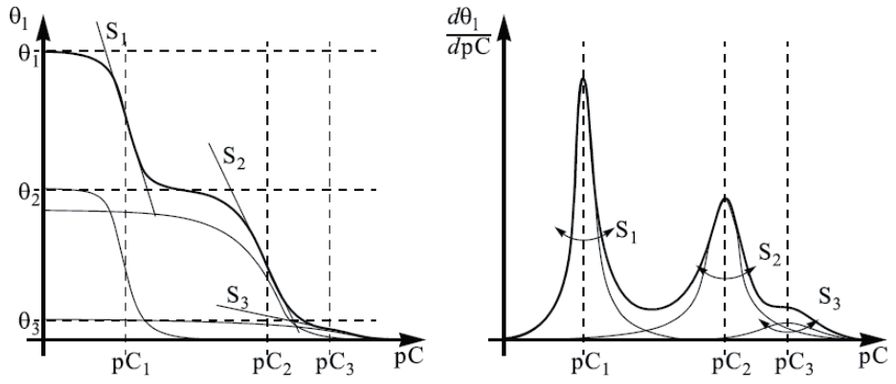

Fig. 1. Three-modal moisture storage function and its derivative, the pores volume distribution. Parameters possess a mathematical meaning and, thus, can be directly determined from measured moisture storage data. The thin lines indicate the influence of each modality. They are summed up in eqs. and resulting in the thick envelope curves.

The moisture storage function $\theta_l(p_c)$ specifies the relationship between moisture content and moisture potential. It is the task of material modeling to provide a set of material functions and adjustment procedures to determine these coefficients based on experimental data.

2.1. Description of moisture storage

Basis of the proposed model is the functional description of the pore structure, i.e. the pore volume distribution or moisture retention characteristic. Due to its high flexibility in adjustment of measured data, a weighted sum of Gauss cumulative distribution functions is chosen following [12]. The moisture storage function is then given by eq. 2 and the pore volume distribution as its derivative by eq. 3. There, the capillary pressure is expressed by $pC = \log(-p_c)$ in a logarithmic scale.

$$\theta_l(pC) = \sum_{i=1}^{N}\left[\frac{\Delta\theta_i}{\sqrt{2}}\left(1+\mathrm{erf}\left(\frac{pC_i - pC}{\sqrt{2}\cdot S_i}\right)\right)\right] \qquad (2)$$

$$\frac{\partial\theta_l}{\partial pC} = -\sum_{i=1}^{N}\left[\frac{\Delta\theta_i}{\sqrt{2\pi}\cdot S_i}\cdot\left(-\frac{(pC - PC_i)^2}{2S_i^2}\right)\right] \qquad (3)$$

Fig. 1 gives an illustration of the parameters contained in eqs. 2 and 3 for a modality of N = 3. The pC_i define the positions of pores maxima, i.e. the inflexion points within the moisture storage function. The slope at these inflexion points is influenced by the S_i. They are the standard deviations in the pores volume distribution function. Finally, the θ_i specify the plateau levels between the different modalities. They represent the weighting factors for each modality and can be obtained according to the following equation:

$$\Delta\theta_i = \theta_i - \theta_{i+1} \quad \text{for} \quad i < N, \quad \text{where} \quad \Delta\theta_N = \theta_N \qquad (4)$$

Alternatively to eqs. and, also other multi-modal functional descriptions could be chosen, as e.g. [8, 14, 28]. However, besides the good flexibility of eq. especially for higher modalities, the direct interpretation of its parameters on the basis of measured data appeared expedient.

It is recommended to adjust the moisture storage function to measured sorption and retention data [26]. Then, the derived pores volume distribution function displays the pores space available to water. Also, or in addition to that, data from image analyzing techniques [23] or mercury intrusion [1, 23] can be used. Note, that moisture sorption and retention data are directly related to the quantity of investigation (water) and might hence be more reliable for use in porosity models. The proposed model is thus based on such data [26], however, not restricted to it.

2.2. Description of moisture transport

It is expedient to first provide the transport coefficients on the basis of what is already available. For vapor transport, it is the general reduction of vapor permeability inside the material due to the increased path length of vapor molecules due to the material's pore structure. For liquid transport, it is the pore model following the bundle of tubes idea. Subsequently, the mechanistic model is being introduced providing contributions to both liquid and vapor transport. Finally, those different parts are combined, the overall procedure is listed and the final transport coefficients are given.

2.2.1. Vapor transport

Vapor transport is typically described by a material specific reduction of the vapor permeability of still air. A number of empirical relations exist for the vapor difusivity in air [10]. The most common expression was found by Schirmer [27] and is given in where p_0 is the reference gas pressure of 101,323 Pa, p is the actual air pressure [Pa] and T is the temperature in [K].

$$D_{v,air} = 0.083\cdot\frac{p_0}{p}\cdot\left(\frac{T}{273.15}\right)^{1.81} \qquad (5)$$

The material specific resistance is obtained by dry-cup and wet-cup vapor diffusion experiments [26]. It is expressed as vapor diffusion resistance factors μ [-]. The dry-cup vapor diffusion resistance fac-

tor μ_{dry} is assumed to comprise vapor transport only. It is used to define the vapor permeability $D_{v,air}$ of the dry material.

$$D_{v,mat} = \frac{D_{v,air}}{\mu_{dry}} \tag{6}$$

The moisture dependency of the vapor diffusion coefficient is related to the reduction of available air-filled pore space with increasing pore filling level. The mechanistic model provides a functional description for this as well. Based on this description, data from wet-cup experiments can be used to derive liquid conductivity data in the hygroscopic moisture range as will be shown later on.

2.2.2. Liquid transport

As the basis for our derivation of the liquid transport function, we employ a bundle of tubes model. Such models follow a simplified representation of the pore structure consisting of a bundle of parallel and interconnected tubes [5, 7]. The laminar flow in a single tube is expressed by the Hagen-Poiseuille equation assigning the volume flow to the tube radius, the dynamic viscosity of the liquid phase and the gradient of the capillary pressure.

To extend this flow description from one tube to a bundle of tubes, this procedure is integrated over the pore radii distribution density. If the pore radius is transformed into the capillary pressure applying the Laplace equation, the integral contains the inverse of the moisture storage function. Since such liquid conductivity overestimates the liquid transport, it is frequently related to its value at saturation. Burdine [5] introduced a tortuosity factor accounting for the tortuosity of flow paths. He proposed to use a value of 2. The relative conductivity can then be scaled by a measured conductivity value at saturation to obtain the absolute conductivity function [20, 21, 28].

We use the principle according to Burdine [5] to derive the liquid conductivity function disregarding the tortuosity factor. Assuming full correlation between different pore bundles, the relative conductivity function is numerically determined from the inverse of the moisture storage function according to the following equation:

$$K_{l,rel}(\theta_l) = \frac{\int_0^{\theta_l} p_c(\theta)^{-2}\,d\theta}{\int_0^{\theta_{eff}} p_c(\theta)^{-2}\,d\theta} \tag{7}$$

$K_{l,rel}$ contains the relative information of the material pore structure. It requires further adjustment since the model displays only a rough approximation of the pore structure.

The pore model describes the liquid water transport in the pore system in a rather simple way. Among others, a completely interconnected liquid phase is assumed which enables a continuous capillary flow. This denotes parallel liquid transport which might indeed apply if most of the pores are water filled. Within the low (hygroscopic) and the low intermediate moisture content range, the liquid phase exists mainly in form of isolated sub-domains which are not or only partly capillary interconnected. They can interact via the gaseous phase only. This process can be described as serial transport which is – in comparison to the parallel transport – more efficient in the gaseous phase, while it is much less powerful in the liquid phase.

The idea of the mechanistic model is based on the distinction of serial and parallel structured pore domains. Applying this to the transport equations of liquid and vapor transport and introducing a moisture content dependency of the ratio of parallel structured pore domains leads to two scaling factors for liquid and vapor transport, respectively. For a detailed description of this model and the derivation of these scaling factors, refer to [24] and [25].

$$f_v(\theta_l) = \frac{1-\frac{\theta_l}{\theta_{por}}}{\left(\frac{\theta_l}{\theta_{por}}\right)^{\eta_{sp}} + \left(1-\frac{\theta_l}{\theta_{por}}\right)^2 \cdot \left(1-\left(\frac{\theta_l}{\theta_{por}}\right)^{\eta_{sp}}\right)} \tag{8}$$

$$f_v(\theta_l) = \frac{\left(\frac{\theta_l}{\theta_{por}}\right)^{\eta_{sp}}}{\left(\frac{\theta_l}{\theta_{por}}\right)^{\eta_{sp}} + \left(1-\frac{\theta_l}{\theta_{por}}\right)^2 \cdot \left(1-\left(\frac{\theta_l}{\theta_{por}}\right)^{\eta_{sp}}\right)} \tag{9}$$

Instead of employing one tortuosity factor, we propose further calibration which includes scaling and coupling with this mechanistic model. This allows to adjust the conductivity function within the whole moisture range with more flexibility than the models of Burdine [5] and Mualem [20].

2.2.3. Resulting vapor permeability

Including the scaling term $fv(\theta_l)$ according to eq. 9 into eq. 5 yields the final vapor transport coefficient given in the following equation:

$$D_{v,mat}(\theta_l) = \frac{D_{v,air}}{\mu_{dry}} \cdot f_v(\theta_l) \tag{10}$$

This vapor permeability is influenced by η_{sp}. However, the influence is of minor impact, see Fig. 2. Note that the abscissa is of normal scale and not, as the conductivity in Fig. 3 and Fig. 4, in logarithmic scale.

Vapor diffusion can occur in any air-filled pore. The vapor permeability is therefore defined for moisture contents between dry and porosity, i.e. total saturation. With increasing moisture content, the vapor permeability decreases which is in accordance to the reduction of pore space available for vapor diffusion.

The maximum of the vapor permeability is a consequence of the mechanistic model accounting for the effect of liquid shortcuts and the correspondingly higher vapor pressures in the gas filled pore space. The parameter η_{sp} can be adjusted by the help of drying data.

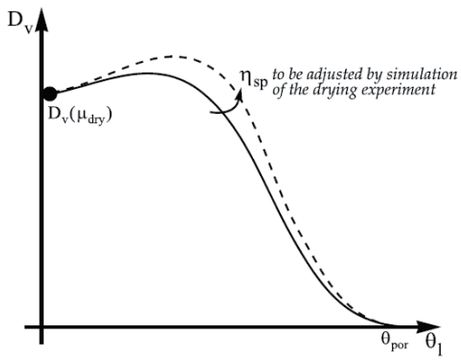

Fig. 2. Vapor diffusivity in dependence of the water content and the parameter η_{sp} from the mechanistic model.

2.2.4. Resulting liquid conductivity

The resulting liquid conductivity is composed of several parts. The core conductivity function is derived from the pore model according to eq. 8. This core function is combined with the liquid scaling factor from the mechanistic model . Then, a general scaling is proposed. Finally, two more steps are introduced to include measured conductivity data in the hygroscopic and the saturated moisture content range. These steps are explained as follows, starting with the incorporation of conductivity data derived from wet-cup vapor diffusion experiments. Illustration is provided in Fig. 3 Wet-cup vapor diffusion experiments comprise conditions where both liquid and vapor transport proceed. Applying eq. 9 to determine the share of vapor transport, it is possible to derive the liquid transport fraction from wet-cup measurements. To obtain conductivity data which is directly associated with the capillary pressure, the vapor permeability D_v associated with the vapor pressure needs to be rewritten in terms of capillary pressure. This is done using Kelvin's law (see eq. (1) in [26]) which leads to K_v according to the following eq.:

$$K_v(\theta_l) = \frac{D_v(\theta_l)}{R_v \cdot T} \cdot \frac{1}{\rho_l} \cdot \frac{\varphi(\theta_l) \cdot p_{v,s}(T)}{R_v \cdot T} \qquad (11)$$

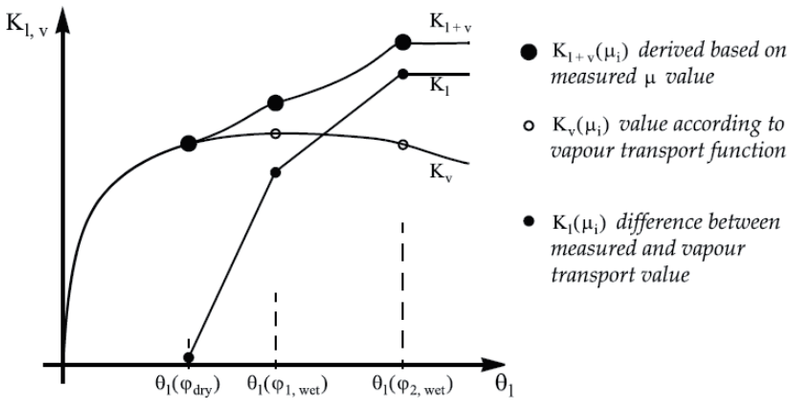

Fig. 3. Determination of the hygroscopic liquid water conductivity as the difference between derived conductivity data from dry-cup and wet-cup measurements and the vapor transport function according to the mechanistic model. The index i denotes different vapor diffusion measurements, in the figure i = 3. Note that the conductivity is plotted in logarithmic scale.

In the same way, the permeability values corresponding to the measured vapor diffusion resistance factors μ are transformed into moisture conductivity values $K_{l+v}(\mu_i)$. Ultimately, from the difference of these measured moisture conductivity values and the derived vapor conductivity, the hygroscopic liquid water conductivity can be determined. This procedure is illustrated in Fig. 3 for three values from cup measurements. The dry-cup value μ_{dry} is regarded to comprise vapor transport only. The vapor permeability is fixed on that point and liquid water transport is supposed to be zero. The hygroscopic liquid water conductivity $K_{l,hyg}(\theta_l)$ is then defined by logarithmic interpolation of the liquid conductivity values obtained from the wet-cup data.

Above capillary saturation, measured conductivity data from permeameter or infiltrometer measurements might be used. If available, the core conductivity function is truncated at capillary saturation θ_{cap} and interpolated with the measured data. Thus the saturated conductivity $K_{l,sat}(\theta_l)$ is determined likewise as the hygroscopic conductivity. In the case when no measured conductivity data are available in the high moisture content range, the conductivity derived by the pore model is applied for the whole moisture content range with an estimated K_{eff} value.

Finally, a general scaling parameter η_{cap} is introduced to adjust the conductivity function in the higher moisture content range. This parameter provides additional flexibility in the moisture range which is particularly important for water absorption processes without having to omit measured conductivity data at saturation. Together with the other components, this leads to the capillary conductivity according to eq. 12 which is valid from dry to capillary saturation θ_{cap}, and the whole liquid conductivity definition according to eq. 13

$$K_{l,cap}(\theta_l) = K_{l,hyg}(\theta_l) + \eta_{cap} \cdot K_{l,rel}(\theta_l) \cdot K_{eff} \cdot f_l(\theta_l) \quad \text{for } \theta_l \le \theta_{cap} \qquad (12)$$

$$K_{l,cap}(\theta_l) = \begin{cases} K_{l,cap}(\theta_l) & \text{if} \quad (\theta_l \le \theta_{cap}) \\ K_{l,sat}(\theta_l) & \text{if} \quad (\theta_l > \theta_{cap}) \end{cases} \qquad (13)$$

As the derivation according to the pore model is typically done numerically, the whole conductivity function is provided in form of data points which are to be logarithmically interpolated for use in simulation. Therefore, the hygroscopic liquid water conductivity is simply added to the derived data. The calibration of the liquid water conductivity function, i.e. the adjustment of the parameters η_{cap} and η_{sp}, is done iteratively by simulation of water absorption and drying experiments. The global scaling factor η_{cap} is to be adjusted based on water absorption data. The parameter η_{sp} from the mechanistic model influences the liquid water conductivity in the lower intermediate moisture range as well as the vapor permeability. It is adjusted on the basis of drying data. See also Fig. 4.

2.3. Overall procedure

The following procedure is proposed to obtain the liquid and vapor transport coefficients. The final

liquid water conductivity includes two adjustable parameters as well as directly measured conductivity data. The final vapor permeability shares one of these adjustable parameters and contains measured vapor diffusion data.

1. Derive the relative liquid conductivity from the moisture storage function by applying the bundle of tubes model .
2. Determine the absolute conductivity function by scaling the relative one to the measured conductivity value K_{eff} at saturation.
3. Determine the vapor permeability according to based on measured dry-cup vapor diffusion data and an initial estimated the mechanistic model parameter η_{sp}.
4. Derive hygroscopic conductivity data $K_{l,hyg}(\theta_l)$ from the difference of the vapor permeability and wet-cup vapor diffusion measurements, and add them to the conductivity function.
5. Introduce a general scaling factor η_{cap} at capillary saturation θ_{cap}. Truncate the conductivity function at capillary saturation and interpolate between the final value $K_l(\theta_{cap})$ and the measured saturated conductivity data from permeameter or infiltrometer experiments.
6. Apply the scaling function $f_l(\theta_l)$ from the mechanistic model according to with an initial estimate for η_{sp}.
7. Optimize both modeling parameters by numerical simulation of the water absorption and the drying experiment. This is an iterative process. η_{cap} is adjusted by the aid of water absorption data, and η_{sp} by the aid of drying data.

3. Example of application

The developed material model has been successfully applied to different porous materials [24]. Based on the measured material data according to [26], the moisture storage function was adjusted for adsorption and desorption, (see Fig. 5).

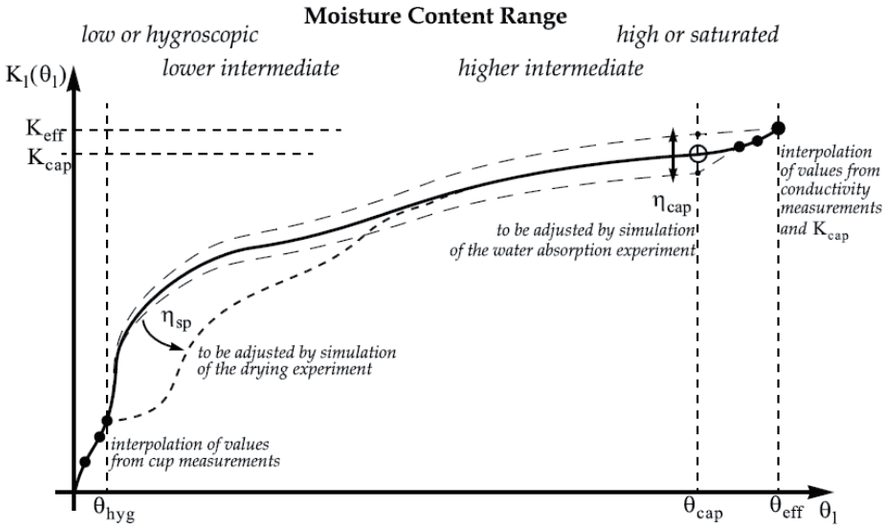

Fig. 4. Calibration of the liquid water conductivity function. Data in the hygroscopic moisture range is derived from cup measurements, data in the saturated moisture range from permeameter or infiltrometer measurements. The slope in between is derived by the bundle of tubes model from the pore structure and can be calibrated adjusting η_{sp} and η_{cap} by the help of numerical simulation.

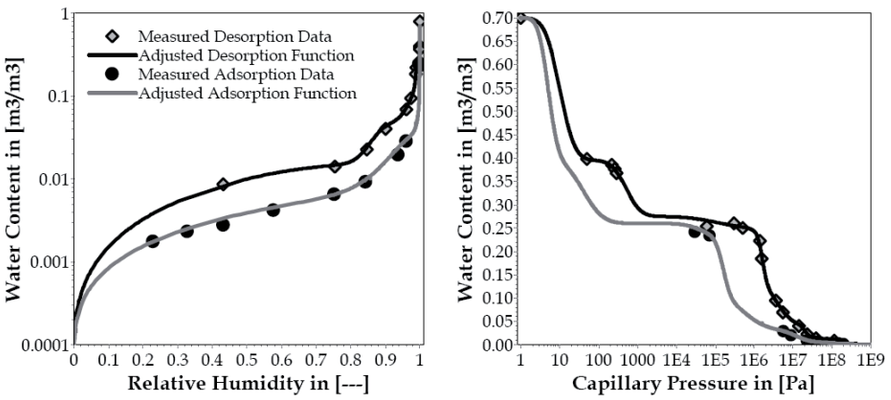

Fig. 5. Desorption and adsorption moisture storage function of aerated autoclaved concrete: sorption isotherm (left) and moisture retention characteristic (right).

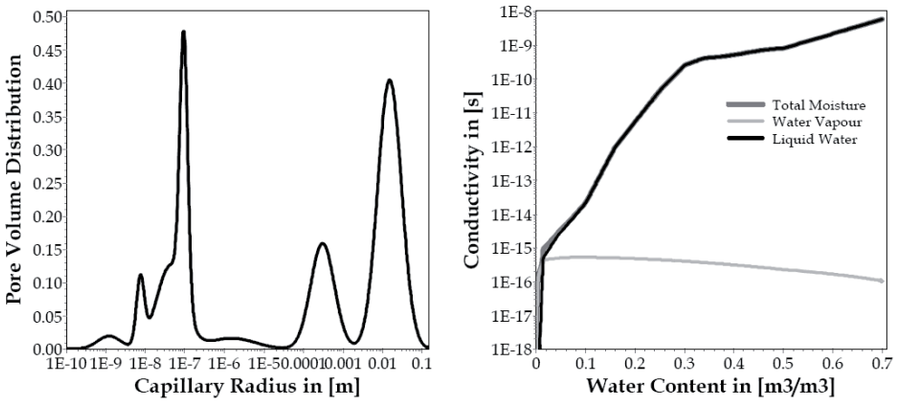

Fig. 6. Aerated autoclaved concrete: pore volume distribution (left) and total moisture conductivity function (right) as the sum of liquid and vapor conductivity.

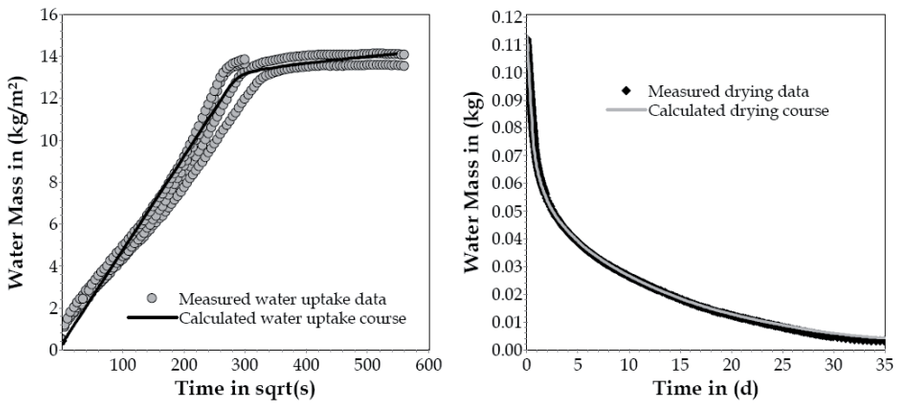

Fig. 7. Calibration of the aerated autoclaved concrete: comparison of measured and simulated courses for water uptake (left) and for drying (right). The drying data was measured with an automatic balance device.

From the desorption moisture storage function shown in Fig. 5, the pore volume distribution function can be derived. It is shown for the AAC in Fig. 6 at the left. Further application of the model leads to the derivation of the liquid conductivity function, shown in Fig. 6 at the right together with the vapor and the total moisture conductivity.

The modeling parameters η_{cap} and η_{sp} were adjusted based on water absorption and drying data. The conductivity function depicted in Fig. 6 is the result of this optimization. Fig. 7 illustrates the accuracy which can be reached. The left chart shows a comparison of measured water absorption data with the calculated behavior. The right chart shows the same for drying. It is apparent that the proposed model is able to reach a perfect agreement between measured and calculated material behavior. The original Burdine model, even if all the other introduced steps are also applied (steps 1–5), does not provide enough flexibility throughout the whole moisture range [25]. The additional flexibility in the adjustment of the liquid conductivity function is required in order to follow both water absorption and drying processes with a high degree of accuracy.

4. Conclusions

The developed material model follows the conductivity approach. Liquid transport is expressed by a conductivity function associated with the capillary pressure gradient, vapor transport is described by a vapor permeability, assigned to the vapor pressure gradient. The main material property is the pore structure either expressed by the moisture storage function or its derivative, the pore volume distribution. Their functional description consists of a sum of weighted (cumulative) distribution functions of the Gauss type which are to be adjusted to measured moisture storage or pore structure data.

The core liquid water conductivity is derived from the moisture storage function applying a bundle of tubes model. It is coupled with a mechanistic model distinguishing between serial and parallel structured moisture transport. This provides two moisture dependent scaling terms, one for liquid and one for vapor transport, respectively. As result, a flexible description of the liquid conductivity is obtained which can be adjusted throughout the whole moisture range based on vapor diffusion, water absorption, drying and saturated permeability data. The resulting vapor permeability is adjusted based on vapor diffusion data.

The model was developed with a focus on porous media with a rigid and open pore system, as e.g. autoclaved aerated concrete. The chosen description of moisture storage has a high flexibility in adjustment to measured data and forms the basis of the liquid transport function. While still rather simple to apply, the model provides a very flexible description of the liquid conductivity. In contrast to other bundle of tubes models, the proposed model allows to adjust the conductivity throughout the whole range of moisture content based on standard moisture transport data from water absorption and drying experiments.

References

[8] J. Adolphs, M.J. Setzer, P. Heine, Changes in pore structure and mercury contact angle of hardened cement paste depending on relative humidity, Mater. Struct. **35** (2002) 477-486.

[9] J. Bear, Y. Bachmat, Introduction to Modeling of Transport Phenomena in Porous Media, Kluwer Academic Publishers, Dordrecht, 1991.

[10] B. Blocken, J. Carmeliet, Spatial and temporal distribution of driving rain on a low-rise building, Wind Struct. **5** (2002) 441-462.

[11] B. Blocken, J. Carmeliet, On the validity of the cosine projection in wind-driven rain calculations on buildings, Build. Environ. **41** (2006) 1182-1189.

[12] N.T. Burdine, Relative permeability calculations from pore-size distribution data, Trans. AIME **198** (1953) 71-78.

[13] D.A. de Vries, The theory of heat and moisture transfer in porous media revisited, Int. J. Heat Mass Transfer **30** (1987) 1343-1350.

[14] F.A.L. Dullien, Porous Media – Fluid Transport and Pore Structure, Academic Press, New York, 1979.

[15] W. Durner, Hydraulic conductivity estimation for soils with heterogeneous pore structure, Water Resour. Res. **30** (1994) 211-223.

[16] C. Finkenstein, P. Häupl, Atmospheric longwave radiation being a climatic boundary condition in hygrothermal building part simulation, in: Proceedings of the 12th Symposium for Building Physics in Dresden, 2007, pp. 617-624.

[17] G.H. Galbraith, Heat and mass transfer within porous building materials, Ph.D. Thesis, University of Strathclyde, Glasgow, 1992.

[18] J. Grunewald, Diffusiver und konvektiver Stoff- und Energietransport in kapillarporösen Baustoffen, Ph.D. Thesis, Dresden Univeristy of Technology, 1997.

[19] J. Grunewald, P. Häupl, M. Bomberg, Towards an engineering model of material characteristics for input to HAM transport simulations. Part 1: an approach, J. Therm. Environ. Build. Sci. **26** (2003) 343-366.

[20] P. Häupl, J. Grunewald, H. Fechner, H. Stopp, Coupled heat air and moisture transfer in building structures, Int. J. Heat Mass Transfer **40** (1997) 1633-1642.

[21] P. Häupl, H. Fechner, Hygric material properties of porous building materials, J. Therm. Environ. Build. Sci. **26** (2003) 259-284.

[22] H. Janssen, The influence of soil moisture transfer on building heat loss via the ground, Ph.D. Thesis, Catholic University of Leuven, 2002.

[23] H. Janssen, B. Blocken, J. Carmeliet, Conservative modelling of the moisture and heat transfer in building components under atmospheric excitation, Int. J. Heat Mass Transfer **50** (2007) 1128-1140.

[24] H. Janssen, B. Blocken, S. Roels, J. Carmeliet, Wind-driven rain as a boundary condition for HAM simulations: analysis of simplified modelling approaches, Build. Environ. **42** (2007) 1555-1567.

[25] H.M. Künzel, Verfahren zur ein- und zweidimensionalen Berechnung des gekoppelten Wärme- und Feuchtetransports in Bauteilen mit einfachen Kennwerten, Ph.D. Thesis, University of Stuttgart, 1994.

[26] H.M. Künzel, K. Kiessl, Calculation of heat and moisture transfer in exposed building components, Int. J. Heat Mass Transfer 40 (1997) 159–167.

[27] Y. Mualem, A new model for predicting the hydraulic conductivity of unsaturated porous media, Water Resour. Res. **12** (1976) 513-522.

[28] Y. Mualem, Modeling the hydraulic conductivity of unsaturated porous media, in: M. Th. van Genuchten, F.J. Leij, L.J. Lund (Eds.), Proceedings of the International Workshop on Indirect Methods for Estimating the Hydraulic Properties of Unsaturated Soils, Riverside, California, October 1989, University of California, 1992.

[29] A. Nicolai, Modeling and numerical simulation of salt transport and phase transitions in unsaturated porous building materials, Ph.D. Thesis, Syracuse University, New York, 2007.

[30] S. Roels, J. Elsen, J. Carmeliet, H. Hens, Characterisation of pore structure by combining mercury porosimetry and micrography, Mater. Struct. **34** (2001) 76-82.

[31] G.A. Scheffler, Validation of hygrothermal material modelling under consideration of the hysteresis of moisture storage, Ph.D. Thesis, Dresden University of Technology, Dresden, 2008.

[32] G.A. Scheffler, R. Plagge 2010. A whole range hygric material model: Modelling liquid and vapour transport properties in porous media. Int. J. Heat Mass Transfer **53** (2010) 286-296.

[33] G.A. Scheffler, R. Plagge 2011. Methods for moisture storage and transport property determination of autoclaved aerated concrete. Article submitted to the 5th International Autoclaved Aerated Concrete Conference in Bydgoszoz, Poland September 2011.

[34] R. Schirmer, Die Diffusionszahl von Wasserdampf-Luftgemischen und die Verdampfungsgeschwindigkeit, VDI Beiheft Verfahrenstechnik **2** (1938) 170-177.

[35] M.T. van Genuchten, A closed-form equation for predicting the hydraulic conductivity of unsaturated soils, Soil Sci. Soc. Am. J. **44** (1980) 892-898.